Gas phases in the Galaxy

component	M ($10^9 M_\odot$)	gas mass fraction
total H II	1.12	23%
total H I	2.9	60%
total H_2	0.84	17%
total gas including He	6.7	-
stars	50	-
dark halo	$\approx 2 \times 10^3$	

- The phases of the ISM behave to a certain degree as phases of a fluid: solid - liquid - gaseous.
- Density (temperature) sets the state of the phase.
- Star forming is exclusively in the H_2 phase.

Star forming regions

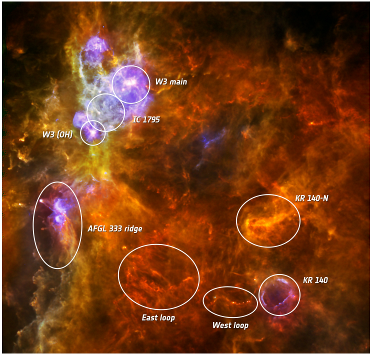

(Rivera-Ingraham et al. 2013)

- In the Galaxy, star formation occurs within molecular clouds.
- Typical mass $10^4 \mathrm{M}_\odot$ to $5 \times 10^6 \mathrm{M}_\odot$; self-gravity.
- Typical scales $5\mathrm{pc}$ to $100\mathrm{pc}$.
- Molecular clouds are turbulent.
- Density typically above $400\mathrm{cm}^{-3}$. Enveloped in H I gas.

Star forming regions

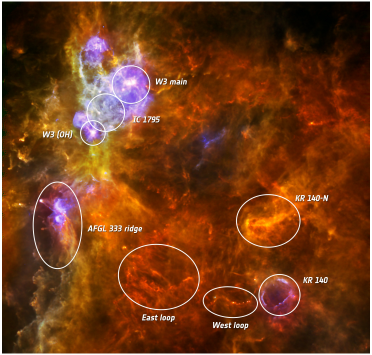

(Rivera-Ingraham et al. 2013)

- Life-time of several Myr. They are transient, they are not long-living objects like many of star clusters.
- Molecular clouds are located in the discs of spiral galaxies, and gas rich dwarf galaxies. They are absent (or scarce) in current lenticular (S0) and elliptical galaxies.

Collapsing clouds

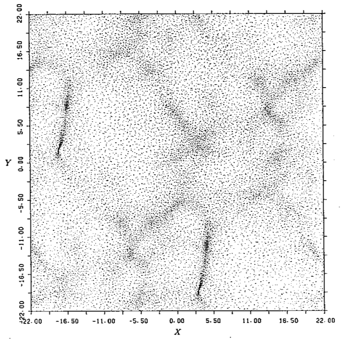

(Miyama et al. 1987)

- Self-gravity is important for collapse of parts of the molecular cloud.
- The collapsing cloud forms an intricated network of sheets and filaments (Herschel space telecope - dust emission).

Collapsing clouds

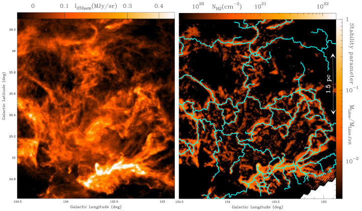

Figure 1. Left: *Herschel*/SPIRE 250 μm dust continuum map of a portion of the Polaris flare translucent cloud ($d \sim 150$ pc) taken as part of the HGBS survey (e.g. Miville-Deschênes et al. 2010, Ward-Thompson et al. 2010). **Right:** Corresponding column density map derived from *Herschel* data (André et al. 2010). The contrast of the filaments has been enhanced using a curvelet transform (cf. Starck et al. 2003). The skeleton of the filament network identified with the DisPerSE algorithm (Sousbie 2011) is shown in light blue. Given the typical filament width ~ 0.1 pc (Arzoumanian et al. 2011 – see Fig. 4 below), this column density map is equivalent to a *map of the mass per unit length along the filaments* (see color scale on the right).

(Andre 2013)

- The situation within a molecular clouds is very different from the idealised spherically symmetric models; flows along filaments.
- Filaments have some remarkable and still elusive properties. E.g. their width is almost universally $0.1\mathrm{pc}$.
- Their density is $\propto \rho_0/(1+(r/r_0)^2)$.
- The majority ($\gtrsim 80$ %) of YSOs are found in filaments; in the field is only their minority.
- Star clusters form at junctions of filaments.

Some properties of filaments

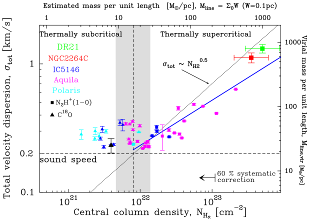

Figure 8. Total (thermal + nonthermal) velocity dispersion versus central column density for a sample of 46 filaments in nearby interstellar clouds (from Arzoumanian et al. 2013). The horizontal dashed line shows the value of the thermal sound speed ~ 0.2 km/s for $T = 10$ K. The vertical grey band marks the border zone between thermally subcritical and thermally supercritical filaments where the observed mass per unit length $M_{\rm line}$ is close to the critical value $M_{\rm line,crit} \sim 16\ M_\odot$/pc for $T = 10$ K. The blue solid line shows the best power-law fit $\sigma_{\rm tot} \propto N_{H_2}{}^{0.36 \pm 0.14}$ to the data points corresponding to supercritical filaments.

(Andre 2013)

- Filaments are observed both in star forming clouds (Aquila rift) and quiescent clouds (Polaris).
- In both regions, the filaments have characteristic radius of $0.1\mathrm{pc}$; however only the ones in Aquila are star forming.
- The line density of filaments decides about their ability to form stars.

Zooming to a filamentary hub

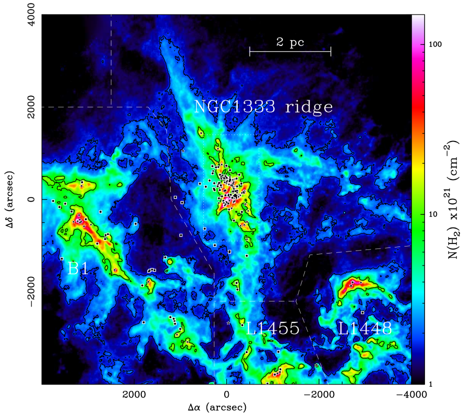

Fig. 1. Large scale view of the NGC1333 ridge in Perseus. The image represents the total column density map derived from our Herschel-Planck maps (in color scale), including two contours of equivalent column densities of $A_V = 2^{mag}$ and 10^{mag}, respectively. Offsets are referred to the map centre with coordinates $(\alpha, \delta)_{J2000} = (03^h29^m08^s.9, +31^\circ15'12'')$ in radio projection. The 4 subregions around NGC1333 and their boundaries are labelled in the plot. The different symbols correspond to the Class 0/I (stars) and Flat/ClassII/III objects (squares) identified by different Spitzer surveys (Gutermuth et al. 2008; Evans et al. 2009). The dotted line encloses the NGC1333 clump studied in this work.

(Hacar et al. 2017)

Zooming to a filamentary hub

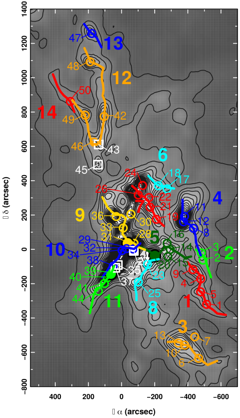

Fig. 16. Core candidates identified in N_2H^+ in NGC1333 (labels 1-50; see Table 5.5). The position of the 44 cores associated to fibers are indicated by open circles and are color-coded similar to Fig. 13c. For reference, the fiber numbers are labeled using a larger font. In addition, the 6 cores found in isolation are marked by white squares. Those cores with masses $M \geq 2.5\ M_\odot$ are highlighted with solid symbols.

(Hacar et al. 2017)

- Filaments consist of fibres; fertile vs. sterile fibres.
- Protostars are found in fibres.
- The vas majority of the youngest protostars (class 0) are found in fibres, while older protostars (classes I-III) are found gradually more dispersed.

Embedded star clusters

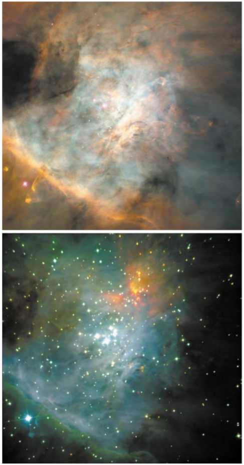

The ONC (Lada & Lada 2003)

- Contain protostars, often main sequence O and B stars but still contain gas.
- More massive stars reach the MS faster.
- Young objects (age $\lesssim$ several Myr).
- Opaque in visible, but much more interesting in the infrared.
- At this time, planets already start forming around stars.

The core mass function and the initial mass function (IMF)

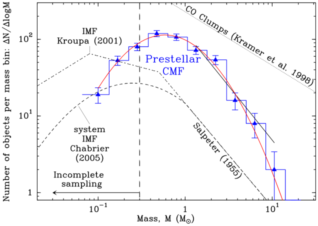

Core mass function (blue histogram with error bars) of the ~ 500 candidate prestellar cores identified with *Herschel* in Aquila (André et al. 2010 and Könyves et al. 2010). The IMF of single stars (corrected for binaries – e.g. Kroupa 2001), the IMF of multiple systems (e.g. Chabrier 2005), and the typical mass spectrum of CO clumps (e.g. Kramer et al. 1998) are shown for comparison. A log-normal fit to the observed CMF is superimposed (red curve); it peaks at $\sim 0.6\,M_\odot$, close to the Jeans mass within marginally critical filaments at $T \sim 10$ K (cf. § 6).

(Alves et al. 2007; Ward-Thompson et al. 2007)

- Mass function tells us how many objects belongs to a given mass bin.

$$\xi(m) \equiv \frac{\mathrm{d}N}{\mathrm{d}m}$$

- Core mass function is shifted by a factor of 3 towards higher masses → might indicate that each core loses ≈ 2/3 of its mass.
- One core might produce more than one star.

The IMF

- Salpeter (1955) found that $\xi(m) \propto m^{-2.35}$ for stars with $4\mathrm{M}_\odot \lesssim m \lesssim 10\mathrm{M}_\odot$.
- This would indicate that there is infinite number of low mass objects $\rightarrow$ cut-off.
- Some refinements came later: Massey 1998, Kroupa 1993, 2001, Chabrier 2005
- E.g. Kroupa 2001 suggests:

$$\frac{\mathrm{d}N}{\mathrm{d}m} = \begin{cases} m^{0.3}, & 0.01\mathrm{M}_\odot \lesssim m \lesssim 0.08\mathrm{M}_\odot \\ m^{1.3}, & 0.08\mathrm{M}_\odot \lesssim m \lesssim 0.5\mathrm{M}_\odot \\ m^{2.3}, & m \gtrsim 0.5\mathrm{M}_\odot. \end{cases}$$

The IMF - some basic numbers

Mass	stellar type	number fraction	mass fraction
$0.01\mathrm{M}_\odot \lesssim m \lesssim 0.08\mathrm{M}_\odot$	brown dwarfs	0.37	0.043
$0.08\mathrm{M}_\odot \lesssim m \lesssim 0.5\mathrm{M}_\odot$	M stars	0.48	0.28
$0.5\mathrm{M}_\odot \lesssim m \lesssim 1\mathrm{M}_\odot$	K stars	0.09	0.17
$1\mathrm{M}_\odot \lesssim m \lesssim 8\mathrm{M}_\odot$	G, F, A, late B	0.06	0.34
$\gtrsim 8\mathrm{M}_\odot$	early B, O	0.004	0.17

- The mean mass of a star is $\langle m \rangle = 0.36\mathrm{M}_\odot$
- The total stellar mass in objects of $m \lesssim 1\mathrm{M}_\odot$ is almost the same as the total stellar mass in objects of $m \gtrsim 1\mathrm{M}_\odot$.

Feedback from young stars

Table 15.1 Ultraviolet Radiation from Massive Stars

Spectral Type	Mass ($M_\odot$)	$\log \mathcal{N}_*$ (s^{-1})	$\log \mathcal{N}_{FUV}$ (s^{-1})
O4	70	49.9	49.5
O5	60	49.4	49.2
O6	40	48.8	48.8
O7	30	48.5	48.6
O8	23	48.2	48.4
O9	20	47.8	48.2
B0	18	47.1	48.1
B1	13	45.4	47.5
B2	10	44.8	47.1

N_* is the number of ionising photons ($E > 13.6\mathrm{eV}$), N_{EUV} is the number of EUV photons ($6\mathrm{eV} < E < 13.6\mathrm{eV}$). (Stahler & Palla 2005)

- Early feedback (occurs immediately after star formation): Photoionising, stellar winds, radiation pressure.
- Late feedback (when the star leaves the main sequence): red supergiant winds, AGB winds, SNe

Simple picture of early feedback bubbles: Photoionising radiation

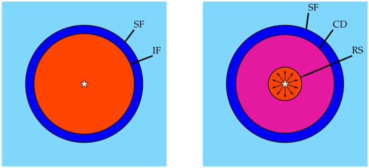

- Photoionising feedback. The bubbles are at temperature of $\approx 10^4\mathrm{K}$ due to an efficient thermostat.
- Cooling via collisional excitation of ions of heavier elements (mainly oxygen, smaller contribution from neon and nitrogen).
- Simple structure: Shock front and ionisation front.

Simple picture of early feedback bubbles: Stellar wind

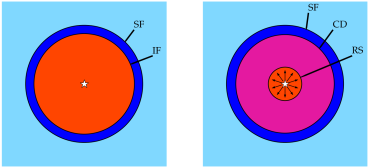

- Free wind region; reverse shock; contact discontinuity; shock front.
- The hot bubble in wind feedback reach temperatures $\gtrsim 10^7\mathrm{K}$.
- Numerical models indicate that the photoionising feedback impacts the interstellar medium more than stellar wind feedback.

The total budget of energy

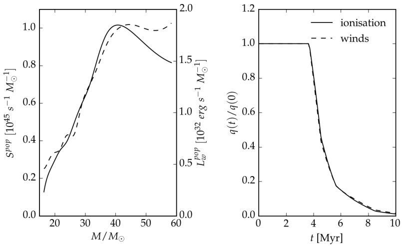

- Energy released by stars of given mass per $1\mathrm{M}_\odot$ of coeval stellar population.
- More massive stars are more numerous, ut they produce the most photons and wind.
- With demise of the most massive stars, feedback energy drops abruptly.

Real picture of early feedback

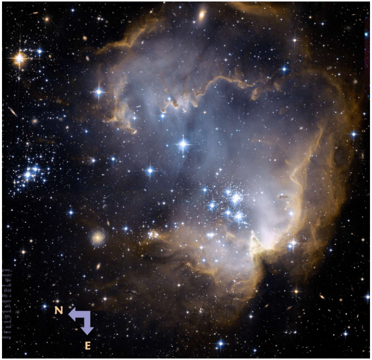

H II region NGC 602

- Don't be confused by distant galaxies.
- Cluster of young stars containing massive stars.
- Gas is being expelled.
- Sharp ionisation front.
- Structures (cones) in the ionisation front.

Late feedback

- Each SN of type II releases suddenly $\approx 10^{51}\mathrm{erg}$.
- SNe are important for shaping the structure of galactic disc, regulate formation of molecular clouds, create the hot phase.
- SNe launch galactic outflows, fountains.
- SNe occur after 3 Myr; the life-time of the most massive stars.
- At the time when SNe occur, embedded clusters have already been cleared by early feedback.

Open Star clusters

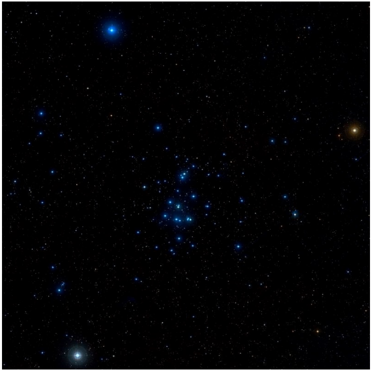

Open star cluster M 44.

- After several Myr, the cluster is gas free.
- Most of open star clusters dissolve early, only 10% of open star clusters reach the age of 10 Myr and 4% reach the age of 100 Myr.
- However, there are some old open star clusters, age up to 10 Gyr (NGC 188, M 67).
- Occupy the disc of the Galaxy.

Open Star clusters

Figure 2

Hubble Space Telescope optical/IR image of the dense massive young cluster R136/30Dor (courtesy of M.J. McCaughrean; FOV ~30 arcsec × 30 arcsec or 7.5 pc × 7.5 pc). Dozens of massive O stars are found crowded within the half-light radius of 2 pc (Brandl et al. 1996). (*a*) A VLT image of NGC 3603 (Brandl et al. 1999) and (*b*) a VLT image of the Trapezium Cluster in Orion (McCaughrean 2001) are shown as these two galactic clusters would be seen if they were located at the distance of R136 in the Large Magellanic Cloud (50 kpc) and imaged with similar angular resolution (see Zinnecker 2002).

Zinnecker & Yorke 2007

- Comparison of sizes of open star clusters.
- (b) ONC - mass $\sim 10^3 \mathrm{M}_\odot$, (a) NGC 3603 - mass $\sim 10^4 \mathrm{M}_\odot$, background: R 136 (in LMC) - mass $\sim 10^5 \mathrm{M}_\odot$.
- Mass ranges from tens of $\mathrm{M}_\odot$ to 10^6 or $10^7 \mathrm{M}_\odot$ in star bursting galaxies (e.g. Antennae).
- Radii are several pc.
- Metallicity is approximately solar $Z_\odot$.

Open Star clusters

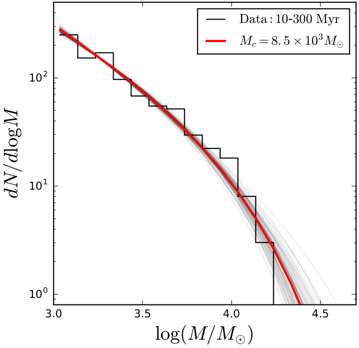

Johnson et al. 2017 (for M 31)

- Cluster initial mass function has a slope of ≈ -2, which is similar to the IMF.
- Slope -2: the same mass of objects in each logarithmic mass bin.
- The most massive clusters are underrepresented.

More massive open star clusters

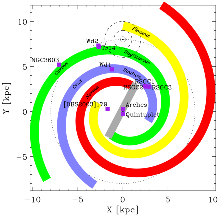

Figure 3: Top view of the Milky Way Galaxy, with the known spiral pattern (Vallée 2008) and young star clusters more massive than $\gtrsim 10^4\,M_\odot$ identified. Basic cluster parameters are listed in Tab. 2. The location of the Sun is indicated by $\odot$, and its orbit by the dotted circle. Dashed lines indicate circles of 1 kpc and 2 kpc around the sun.

(Zwart et al. 2010)

- Distribution of massive open star clusters within the Galaxy.
- The most massive open star clusters currently forming in the Galaxy are of the mass $1 - 2.10^4 M_\odot$.
- Clusters are at the tip of the bar, galactic centre, but also in the disc at relatively large $R_{\rm gal}$.

Massive stars in star clusters

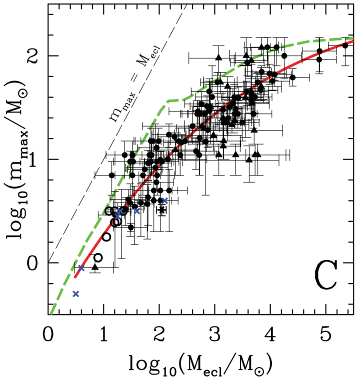

Weidner et al. 2013

- Massive stars are usually found only in the most massive star clusters.
- Perhaps, massive stars need special (high density, pressure) environment to form.
- Massive stars are often found mass segregated, i.e. more massive stars are found closer to the cluster centre.
- Mass segregation can be primordial or dynamical.

Theories for open star cluster formation

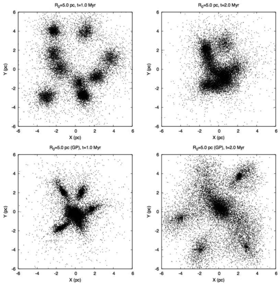

Figure 7. Evolution for the 'extended' system A-IIId ($R_0 = 5$ pc, see Table 3). As expected, the infall of the subclusters proceeds much more slowly than that for the compact systems (cf. Figs 4). The system is still highly substructured (SUB) at $t \approx 2.0$ Myr both in absence (panels 1,2, numbered left-to-right, top-to-bottom) and presence (panels 3,4) of a gas potential. In presence of the gas potential, the subclusters are close to the first arrival at their pericentres (i.e. $t \approx t_{\rm in}$, see Section 3.1) at $t \approx 1$ Myr (panel 3) while this takes $t \approx 2$ Myr without the gas (panel 2). This is consistent with Fig. 3. For the evolution with gas potential, the subclusters make their first passage through each other during 1–2 Myr which is why their configuration at 2 Myr (panel 4) is more extended than that in 1 Myr (panel 3). Note that the gas potential tidally elongates the subclusters significantly (also see Fig. 8).

(Banerjee & Kroupa 2015)

- Formation of star clusters is not well understood.
- Two classes of models: coalescence of subclusters; monolithic scenario.
- Coalescence of subclusters leaves signatures in the merged objects, and constraints the possible compactness of subclusters.

Theories of open star cluster formation

- Competitive accretion (in monolithic star cluster formation; Bonnell et al. 1997).
- Consider a gaseous cloud containing protostars, each protostar is of the same mass.
- Some protostars are located at denser medium, move at different relative velocities $\rightarrow$ different accretion rates.
- Protostars accreting more lose their momentum $\rightarrow$ sink towards the cluster centre $\rightarrow$ are located at denser medium $\rightarrow$ accrete at even higher rate.
- Competitive accretion naturally explains mass segregation as most massive stars are slowed down at the cluster centre.

Binary stars in open star clusters

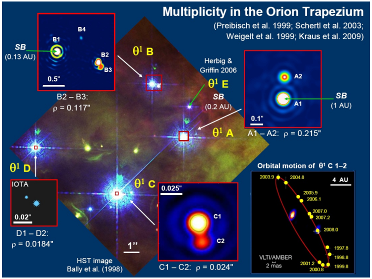

The Trapezium in the Orion Nebula Cluster (ONC)

- Multiplicity increases with the mass of the primary: O stars - 2.1; early B stars - 1.6; A stars - 0.9; G stars - 0.5.
- More massive stars are found in tighter binaries.
- The presence of binary stars is important dynamically.

Binary stars in open star clusters

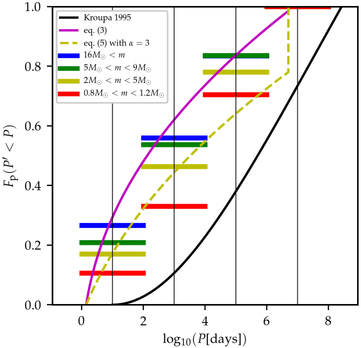

The distribution of orbital periods for stars of various masses (spectral types).

- Multiplicity increases with the mass of the primary: O stars - 2.1; early B stars - 1.6; A stars - 0.9; G stars - 0.5.
- More massive stars are found in tighter binaries.
- The presence of binary stars is important dynamically.

OB associations

- Gravitationally unbound objects, usually expanding.
- Typical size $50\mathrm{pc}$.
- Contain O, B stars, but also lower mass stars (T associations).
- Two possibilities of their origin: expanding outer halos of open star clusters after gas expulsion; formed throughout a molecular cloud, were never gravitationally bound together.
- OB associations are associated with the so called runaway phenomenon $\rightarrow$ almost any association has some runaway stars.

Globular star clusters

- Very different from open star clusters.
- The SFR per unit volume in the cosmic history peaked at $z = 2$ (10 Gyr ago).
- Very old objects, age $\approx$ 12 Gyr.
- Typical mass is 10^4 to $10^6 \mathrm{M}_{\odot}$.
- Almost spherically symmetric, of coeval age.
- But not that "simple" might not be appropriate: multiple stellar populations; their formation.
- Dynamically old ($\sim 10^4$ orbits), they provide nice examples for N-body problem.
- Located in galactic halo, often at eccentric orbits.
- Denser (radii $\approx 3\mathrm{pc}$) than open star clusters.
- Of subsolar metallicity (typically $Z = -2$ to $Z = -0.8$).

Nuclear star clusters

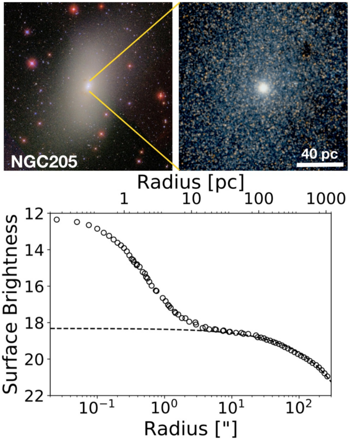

Neumeyer et al. 2020

- Very different from the previous two cases.
- Very dense systems $\sim 10^6 \mathrm{M}_\odot \mathrm{pc}^{-3}$, old.
- In some cases, there is possible interaction with the supermassive black hole.
- Hosted mostly by galaxies of stellar mass 10^8 to $10^{10} \mathrm{M}_\odot$.

Illustration of thermodynamics of self-gravitating systems

- Consider a cluster composed of N stars, each of the same mass.
- A temperature at position r is defined as

$$\frac{1}{2}m\langle v^2(r)\rangle = \frac{3}{2}k_B T(r) \tag{1}$$

- The mean temperature of the cluster is then

$$\overline{T} = \frac{\int 4\pi r^2 \rho(r) T(r) \mathrm{d}r}{\int 4\pi r^2 \rho(r) \mathrm{d}r} \tag{2}$$

- From the virial theorem ($2K + W = 0$), it follows

$$E = -\frac{3}{2}Nk_B\overline{T}. \tag{3}$$

Illustration of thermodynamics of self-gravitating systems

- This implies that the heat capacity is

$$C \equiv \frac{\mathrm{d}E}{\mathrm{d}\overline{T}} = -\frac{3}{2} N k_B. \tag{4}$$

- The heat capacity is negative.
- If we transfer a small amount of heat from the system, the system gets hotter $\rightarrow$ releases heat $\rightarrow$ gets hotter further.
- There is no equilibrium in such a simple model.
- Binary stars stop the collapse.
- Evolved clusters tend to form bound cores with high velocity dispersion enveloped in a low density halos.

Evolution of star clusters

- Relevant for open star clusters (some similarities to globular star clusters, but we do not know how the initial conditions of their formation).
- Early gas expulsion.
- Evaporation and ejections.
- Core collapse.
- Dissolution in the external field of the galaxy.
- Characteristic time-scales are usually expressed in the relaxation time

$$t_{\rm rlx} = \frac{0.34\sigma^3}{G^2 m\rho \log\Lambda}. \tag{5}$$

Early gas expulsion

- Large difference between the adiabatic and impulsive approximation, they depend on the time-scale.
- $t_{\rm cross} < t_{\rm ge} \rightarrow$ adiabatic. Adiabatic invariants (e.g. $aM_{\rm cl}$) are conserved.
- During impulsive gas expulsion, star clusters are typically impacted more.
- Gas expulsion leads to cluster expansion, and many stars (approx. 1/2 to 2/3) are lost for the star formation efficiency of 30%.

Further evolution

- Core collapse occurs at typically $16 t_{\rm rlx}$.
- Clusters are dissolved at typically $20 - 60 t_{\rm rlx}$, depending on the strength of the external field of the galaxy.
- $$r_{\rm t} \simeq R_{\rm gal}(M_{\rm cl}/3M_{\rm gal})^{1/3}. \tag{6}$$
- The presence of the external gravitational field facilitates cluster evaporation.
- During evaporation, clusters lose preferentially lower mass stars, they tend to retain compact remnants (WDs, NSs).

Runaway stars

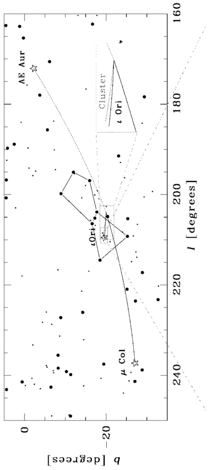

Runaway stars originating from the ONC.

- Runaway stars move at velocity $\gtrsim 30 \mathrm{km\,s^{-1}}$.
- Can be produced by two mechanisms: Close interaction between three or more stars; binary supernova scenario.
- In the binary supernova scenario, the observed star is the former secondary in a binary. When the SN exploded, it decreased suddenly its mass, and also the NS might get a kick.